

Early Sharp Wave Synchronization along the Septo-Temporal Axis of the Neonatal Rat Hippocampus

G. Valeeva,¹ V. Rychkova,¹ D. Vinokurova,¹
A. Nasretdinov,¹ and R. Khazipov^{1,2}

UDC 611.813.14, 611.81.013

Published in Zhurnal Vyssei Nervnoi Deyatel'nosti imeni I. P. Pavlova, Vol. 70, No. 3, pp. 341–350, May–June, 2020. Original article submitted August 1, 2019. Revised version received August 25, 2019. Accepted September 16, 2019.

In the neonatal rat hippocampus, the first and predominant pattern of synchronized neuronal network activity is early sharp waves (eSPWs) occurring at a frequency of ~2–4 events per minute. However, how eSPWs are organized longitudinally along the septo-temporal hippocampal axis remains unknown. Using silicone probe recordings from the septal and intermediate segments of the CA1 hippocampus in neonatal rats *in vivo* we found that eSPWs are highly synchronized longitudinally. The amplitudes of eSPWs in the septal and intermediate segments of the hippocampus were also highly correlated. eSPWs also supported longitudinal synchronization of CA1 multiple unit activity. Spatial-temporal analysis revealed a septal-temporal gradient with more frequent initiation of eSPWs in the septal regions. The speed of eSPW longitudinal propagation attained ~250 mm/s. We suggest that longitudinal correlated activity supported by synchronized eSPWs emerges early during postnatal development and may participate in the formation of intrahippocampal connections in the developing hippocampus.

Keywords: hippocampus, neonate, sharp waves, synchronization.

Early Sharp Waves (eSPWs) are the earliest pattern of synchronized activity in the developing rodent hippocampus considered as a prototype of SPWs in adults [Karlsson et al., 2006; Leinekugel et al., 2002; Marguet et al., 2015; Mohns et al., 2007; Mohns, Blumberg, 2008; Valeeva et al., 2019a; Buzsaki, 2015]. Similarly to the SPW-ripple complexes in adults [Buzsaki, 2015; Csicsvari et al., 2000; Ylinen et al., 1995], eSPWs are associated with a short-lasting negative local field potential deflection below the CA1 pyramidal cell layer, massive activation of synaptic inputs and collective neuronal discharge in the hippocampal network [Karlsson et al., 2006; Leinekugel et al., 2002; Marguet et al., 2015; Mohns et al., 2007; Mohns, Blumberg, 2008; Valeeva et al., 2019a;

Valeeva et al., 2019b]. Yet, despite the similarities in general electrographic phenotype, eSPWs display some unique features different from adult SPWs. For example, eSPWs lack the high-frequency ripple oscillations that are characteristic of adult SPWs [Buhl, Buzsaki, 2005]. Also, eSPWs are reliably triggered by myoclonic movements of neonatal animals, whereas in adults, SPWs, which mainly occur during sleep and periods of immobility, are not associated with movements of the animal [Buzsaki, 2015; Karlsson et al., 2006; Marguet et al., 2015; Valeeva et al., 2019a]. Generation of eSPWs involves activation of entorhinal inputs to the hippocampus suggesting that eSPWs are bottom-up network events embedded into large scale signaling by sensory feedback from neonatal movements [Valeeva et al., 2019a]. In contrast, adult SPWs are a typical top-down signal which is internally generated in the hippocampal network and which enable transfer of the time-compressed replay of neuronal sequences learned during exploration from the hippocampus to the neocortex where memories are consolidated [Buzsaki, 2015; Chrobak, Buzsaki, 1994; Ylinen et al., 1995].

¹Laboratory of Neurobiology, Kazan Federal University, Kazan, Russia.

²Aix-Marseille University, Institut de Neurobiologie de la Méditerranée, Institut National de la Santé et de la Recherche Médicale, Marseille, France;
e-mail: roustem.khazipov@inserm.fr.

Understanding the network mechanisms and physiological roles of eSPWs in the development of hippocampal networks requires knowledge about the spatiotemporal organization of activity in entire hippocampal system. Previous studies revealed that eSWPs support remarkably high levels of bilateral interhemispheric synchronization of neuronal activity in the left and right hippocampi [Valeeva et al., 2019b] which is also characteristic of adult SPWs [Suzuki, Smith, 1987; Buzsaki, 1989; Buzsaki, 2015]. Adult SPWs also show high synchrony levels along the longitudinal septo-temporal hippocampal axis [Chrobak, Buzsaki, 1996; Patel et al., 2013]. While each part of the adult hippocampus is able to generate SPW-Ripple complexes that further propagate towards its septal or temporal side at a rate of ~ 350 mm/s, full SPW propagation along the entire hippocampus is rare and characteristic of large-amplitude SPWs. Small-amplitude SPWs display a more local nature [Patel et al., 2013]. In contrast, spatiotemporal organization of hippocampal activity during eSPWs in neonatal animals along the septo-temporal hippocampal axis remains largely unknown.

The only available knowledge on the septal-temporal organization of activity in the developing hippocampus is based on results obtained using isolated intact hippocampus preparations *in vitro*. Multisite recordings along the septo-temporal axis of the *in toto* neonatal hippocampus preparation revealed that the vast majority of giant depolarizing potentials (GDPs), network activity bursts considered as an *in vitro* analogue of SPWs, are generated in the most septal part and propagate slowly at a speed of 7–10 mm/s towards the temporal end of the hippocampus [Leinekugel et al., 1998]. In keeping with this septal-temporal gradient in GDP propagation, isolated segments of the hippocampus were able to generate GDPs with the highest frequency of generation in the septal segments [Leinekugel et al., 1998]. However, to what extent these septal-temporal gradients and the slow propagation velocity of GDPs in the intact hippocampus *in vitro* are characteristic of eSPWs in rat pups *in vivo* remains unknown.

Here, we addressed the spatio-temporal properties of eSPWs along the longitudinal axis of the hippocampus in neonatal rats *in vivo*. With this aim, we performed field potential and multiple unit recordings from the septal and intermediate hippocampal segments of head-restrained non-anesthetized neonatal rats using multisite silicone probes.

Methods. This work was carried out in accordance with EU Directive 2010/63/EU for animal experiments and all animal-use protocols were approved by the French National Institute of Health and Medical Research (INSERM, protocol N007.08.01) and Kazan Federal University on the use of laboratory animals (ethical approval by the Institutional Animal Care and Use Committee of Kazan State Medical University N9-2013).

Wistar rats of either sex from postnatal days (P) 5–7 from in-house breeding colony were used. Preparation of the animals for recordings was performed under deep iso-

flurane anesthesia the day before recording as previously described [Akhmetshina et al., 2016; Valeeva et al., 2019a]. Recordings were performed from head-restrained non-anesthetized rats. A metal ring was fixed to the skull with dental cement and via ball-joint to a magnetic stand. Animals were surrounded by a cotton nest and heated via a thermal pad (35–37°C) throughout the recording session.

Extracellular recordings of local field potentials (LFPs) and multiple unit activity (MUA) were performed along the CA1 – dentate gyrus axis of the dorsal and intermediate segments of the hippocampus using a pair of 16-site linear silicon probes with 50 μ m separation distance between the electrodes (five animals) or an eight-shank 64-site probe with 200 μ m separation distance (one animal; NeuroNexus, Ann Arbor, MI, USA). DiI coated silicone probes were placed using stereotaxic coordinates [Khazipov et al., 2015]: the septal probe and the first shank of the array were located 1.8–1.9 mm AP, and the intermediate probe – 2.3–2.4 mm AP. Eight shanks of the array were inserted parallel with the septo-temporal axis of the hippocampus. Bare 1.5 mm long chlorided silver wire inserted into the occipital or frontal cortex served as a ground electrode. Signals from extracellular recordings were amplified and filtered (10000 \times ; 0.15–10 kHz) using a DigitalLynxSX amplifier (Neuralynx, Bozeman, MT, USA) and digitized at 32 kHz. From 30 min to an hour of spontaneous activity were recorded in each animal.

After recordings the animals were deeply anesthetized with urethane (3 g/kg, intraperitoneally) and perfused intracardially with 4% paraformaldehyde and 1% glutaraldehyde (Sigma). The brains were removed and left for fixation for a few days. One hundred micrometer-thick coronal slices were cut using a Vibratome (Thermo Fisher Scientific, Waltham, MA, USA). Electrode positions were identified from the DiI tracks overlaid on the microphotographs of sections after cresyl violet staining.

Wideband recordings were preprocessed using custom-written functions in MATLAB (MathWorks, Natick, MA, USA). eSPWs were detected semi-automatically from down-sampled (1000 Hz), bandpass filtered (3–100 Hz, digital RC filter) LFP signals. All events reaching an amplitude greater than 1.5 standard deviations of the filtered LFP on sl-m and pcl channels (negative and positive peaks, respectively) were first considered as putative eSPWs. To discard movement and static artifacts, LFP segments from –1 s to 1 s around the eSPW were visually inspected. The eSPW onset was defined as the time when the first LFP derivative in sl-m reached a threshold of 2 mV/s. Raw data were filtered using a 250–4000 Hz bandpass wavelet filter (Daubechies 4) and spikes were detected as negative events exceeding –3.5 standard deviations of the filtered signal. Time lags were calculated from peri-onset time histograms as described previously [Valeeva et al., 2019a].

Statistical analysis was performed using the MATLAB Statistics toolbox. Group comparisons were done using one- and paired-sample Wilcoxon signed-rank tests. P-value of

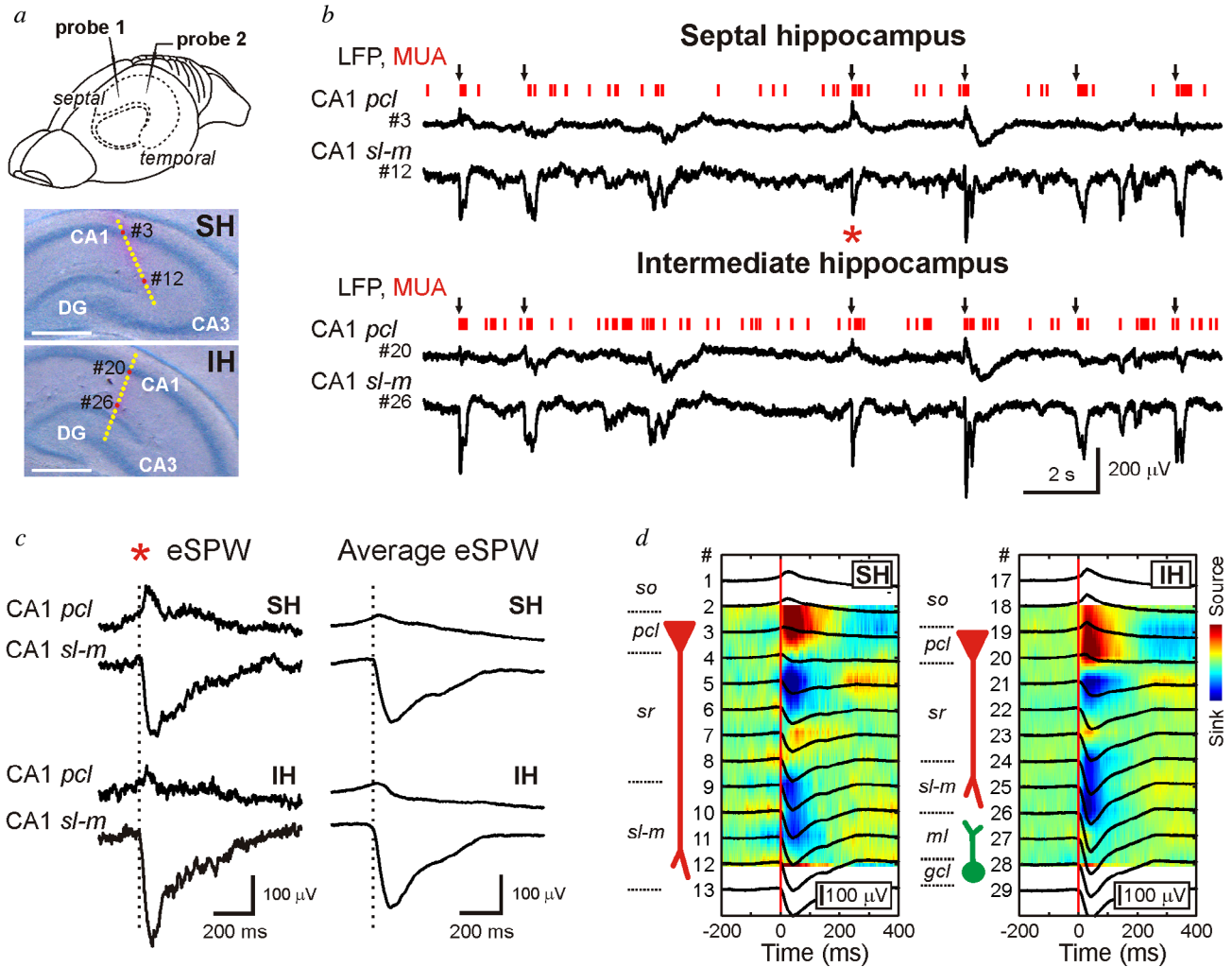


Fig. 1. Co-occurrence of eSPWs in the septal and intermediate hippocampus of neonatal rats. *a*) Top: a schema of recording probes location in the left hippocampus of a rat pup. Middle–bottom: recording sites of 16-channel probes overlaid on a cresyl violet stained coronal slices of the septal (SH, middle) and intermediate (IH, bottom) hippocampal segments. Scale bars, 0.5 mm. *b*) Simultaneous LFP and MUA recordings from the CA1 pyramidal cell layer (pcl, recording sites #3 and #20 on panel *a*) and str. lacunosum-moleculare (sl-m, recording sites #12 and #26 on panel *a*) of the septal and intermediate hippocampal segments. Black arrows above the traces indicate eSPWs. *c*) The eSPW from panel *b* (red asterisk) and average septal eSPW-triggered LFP in the septal and intermediate hippocampus on an expanded time scale. *d*) Septal hippocampal segment eSPWs-triggered LFPs (black) in the septal and intermediate hippocampal segments overlaid on CSD maps.

less than 0.05 was considered significant. Correlations between variables were estimated using the Spearman (*r*) correlation coefficients. Unless indicated, data are presented as mean ± SD.

Results. Local field potential and multiple unit activity were recorded simultaneously from the septal and intermediate segments of the left hippocampus in six P5-7 neonatal rats. The septal and intermediate recording sites were located in CA1 and spaced apart by a distance of 1.2–2.4 mm along the longitudinal hippocampal axis (Fig. 1, *a*). In accordance with previous studies, eSPWs recorded at both sites had similar depth profiles with characteristic current sinks in s. radiatum (sr) and s. lacunosum-moleculare (sl-m) and were associated with pronounced neuronal firing in the CA1 pyramidal layer [Valeeva et al., 2019a] (Fig. 1, *b–d*).

We found that about $94 \pm 3\%$ of eSPWs co-occurred at septal and intermediate hippocampal segments. eSPWs recorded at septal and intermediate sites also well-correlated in amplitude with an average Spearman’s *r* value of 0.76 ± 0.14 ($n = 6$; $p < 0.001$; Fig. 2).

Nearly half of eSPWs ($44 \pm 11\%$) occurred largely synchronously in both segments with a time lag between the onsets of LFP negativity during eSPW of ≤ 3 ms (1.7 ± 0.1 ms average delay of eSPWs in the intermediate segment from the septal segment; $n = 6$ rats; Fig. 3). In $32 \pm 9\%$ of cases, eSPWs appeared first in the septal segment and propagated to the intermediate segment with a 17.4 ± 4.3 ms delay ($n = 6$). In $24 \pm 10\%$ of paired events, eSPWs first emerged in the intermediate segment followed by eSPWs in the septal segment with an 18.2 ± 3.4 ms delay ($n = 6$). Therefore,

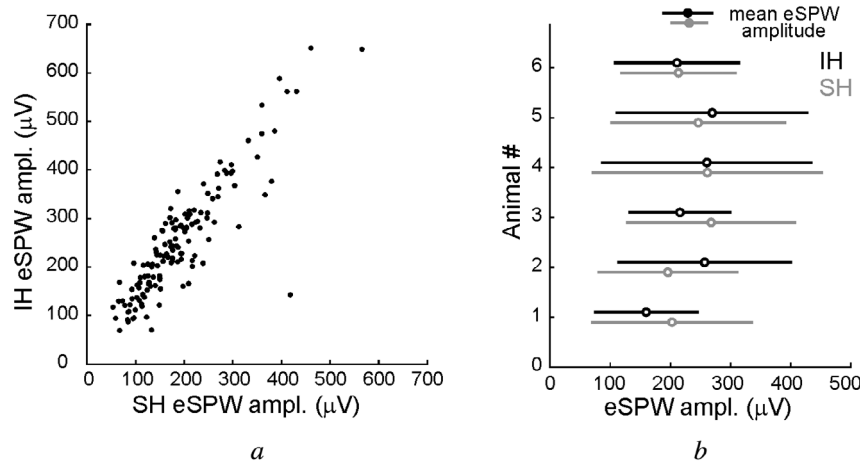


Fig. 2. Relationships between the amplitudes of eSPWs in the septal and intermediate hippocampal segments. *a*) Relationships between eSPW amplitudes recorded in CA1 s-lm layer of septal and intermediate hippocampal segments of a P6 rat. *b*) Amplitude averages of eSPWs in the septal (gray) and intermediate (black) hippocampus of six P5-7 rats (open circles) and group values (closed circles). Error bars show SD.

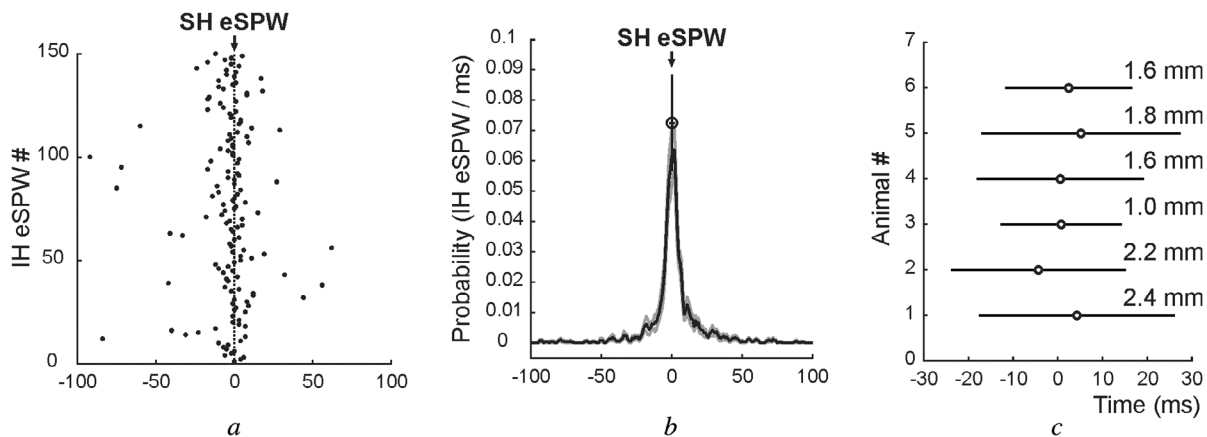


Fig. 3. Temporal relationships between eSPWs recorded in the septal and intermediate hippocampal segments. *a*) Septal eSPW onset-triggered raster plot of intermediate eSPW onsets presented for an individual animal. *b*) Septal segment eSPW onset-triggered normalized PETH of intermediate eSPW onsets. Group average (open circle; mean \pm SD; $n = 6$ animals) show the peak value of normalized PETH and the time lag between septal and intermediate eSPWs. *c*) Average time lags between eSPWs in the septal and intermediate hippocampal segments in six P5-7 rats. Error bars show SD. Distance between two recording sites along the septal-temporal hippocampal axis is shown for each animal on the right.

most frequently eSPWs co-occurred synchronously along the septal/intermediate hippocampal segments, but could also propagate in either the septal-temporal or temporal-septal direction.

We further attempted to estimate the probability of eSPW initiation and speed propagation along the septo-temporal axis (Fig. 4). Knowing the stereotaxic coordinates and taking into account the position of the electrodes in serial sections during histological analysis we first calculated electrode position along the hippocampus. A total longitudinal hippocampal length (L) of ~ 7 mm was measured in the hippocampus isolated from age-matched animals. Electrodes in the septal segment were situated at a distance of 1.53 ± 0.08 mm from the most septal end of hippocampus, whereas the electrodes in the intermediate hippocampal segment were situated at distance of 1.78 ± 0.49 mm

from the electrodes in the septal segment and at a distance of 3.69 ± 0.56 mm from the most temporal end of hippocampus. On average, $22 \pm 1\%$ of the hippocampus was situated septally from the electrodes in the septal segment (distance A), $25 \pm 7\%$ of the hippocampus was situated between the electrodes (distance B), and $53 \pm 8\%$ of the hippocampus was temporal to the electrode in the intermediate segment (distance C) (Fig. 4, *a*). We further assumed that eSPWs can be randomly initiated along the hippocampus and that they fully propagate from the site of initiation septally and temporally along the entire hippocampal length. According to this assumption eSPWs with the shortest delays are presumably initiated in between the electrodes and their percentile estimated as a B/L fraction (0.25 ± 0.07) of all eSPWs was $30 \pm 9\%$ with the delays in a time window of $< 2 \pm 1$ ms. The remaining eSPWs were initiated in the

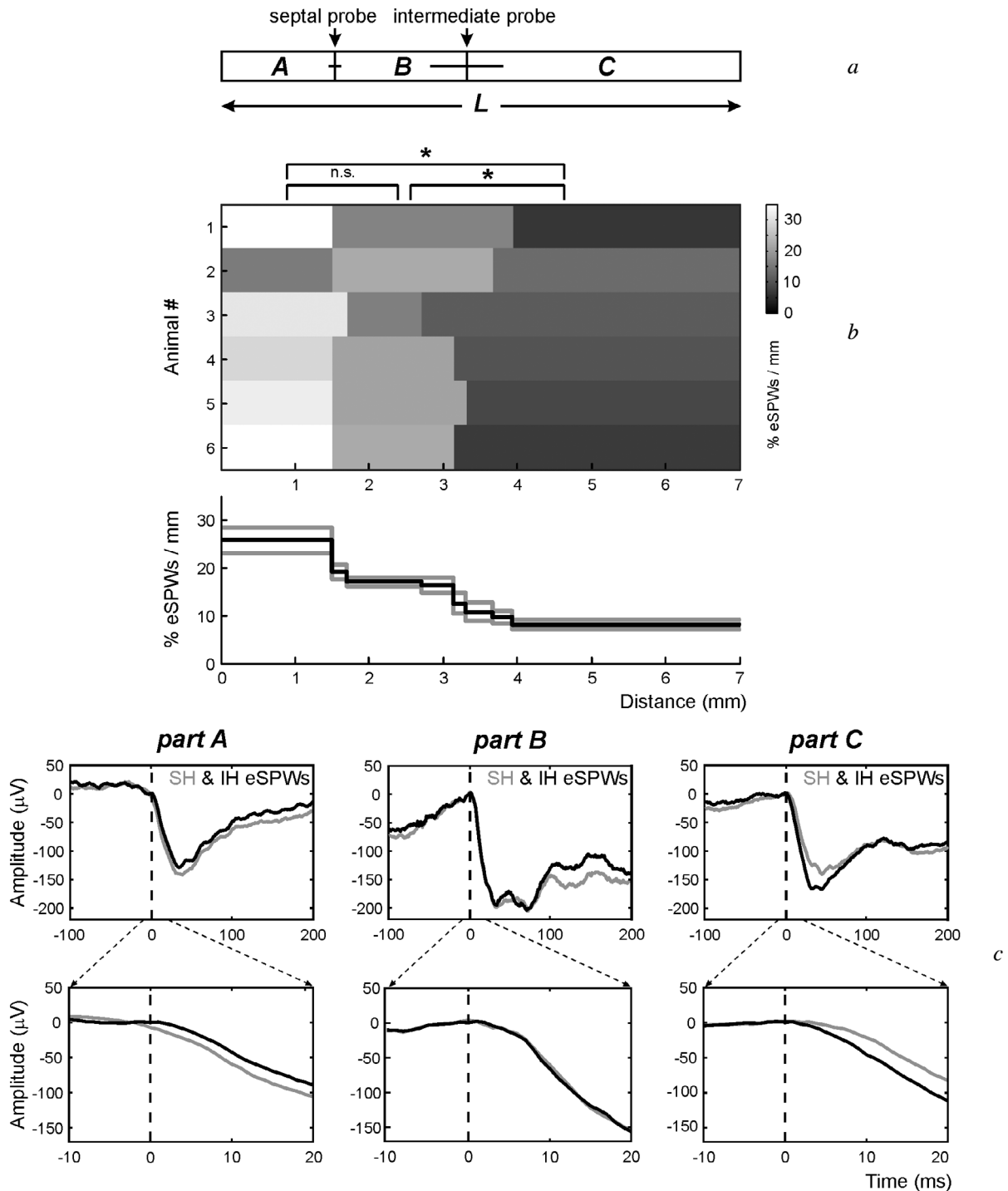


Fig. 4. Estimates of eSPW initiation along the septal-temporal hippocampal axis. *a*) A scheme of septal and intermediate probe locations along the septal-temporal hippocampal axis. The arrows point to average coordinate values with horizontal bars showing SD calculated across 6 animals. The probe positions divide the full length of hippocampus (L) into three parts: the septal part – distance A, distance B between the two probes and distance C, temporal to the intermediate probe. *b*) Top, colour coded probability of eSPWs initiation in the parts A, B, and C normalized to the length of each part in six P5-7 rats. Bottom, average eSPW initiation probability in different parts along the septal-temporal hippocampal axis. Gray lines indicate SE. *c*) Example traces of LFP averages in CA1 sl-m of septal and intermediate hippocampal segments during eSPWs initiated in parts A, B, and C. For each group, LFPs were averaged over 10–50 eSPWs recorded from a P7 rat. Bottom plots show traces around the eSPW onset on an expanded time scale.

more septal part A ($40 \pm 10\%$) and the more temporal part C ($30 \pm 9\%$). After correction of these values for the length of parts A, B, and C, we further estimated that the proba-

bility of eSPW initiation in these parts attained $26 \pm 7\%/mm$, $17 \pm 2\%/mm$, and $8 \pm 2\%/mm$, respectively (Fig. 4, *b*). These results suggest a septal-temporal gradient in eSPW

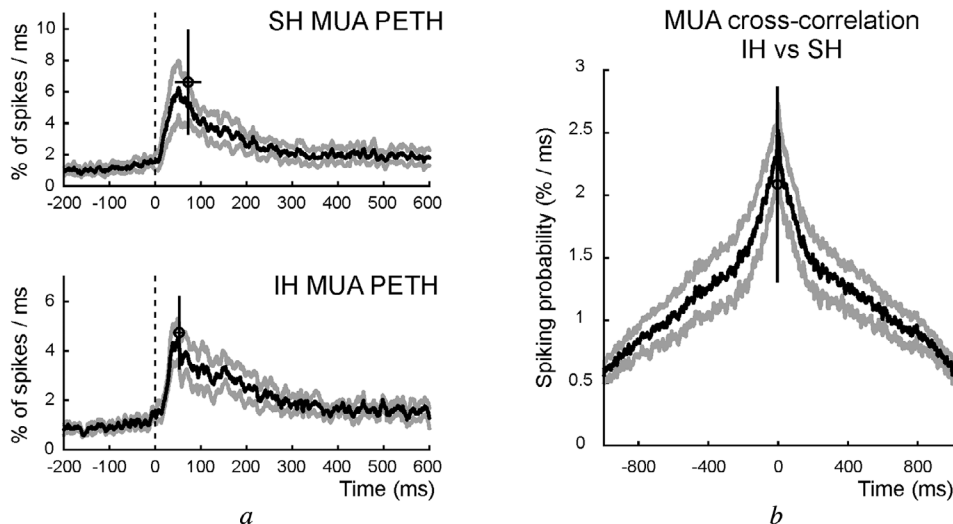


Fig. 5. Longitudinal synchronization of CA1 multiple unit activity during eSPWs. *a*) Septal hippocampal segment eSPW onset-triggered MUA PETHs in septal and intermediate hippocampal segments. Average values are shown by open circles, bars show SD. *b*) Normalized MUA cross-correlogram in intermediate vs. septal hippocampal segments within the time window of eSPWs. *a*, *b*) Group averages from 4 animals. Gray lines show standard errors.

initiation that is in keeping with the results obtained previously in the intact hippocampus in vitro [Leinekugel et al., 1998].

We further estimated the speed of eSPW propagation in the septal-temporal and temporal-septal directions from the delays of eSPWs initiated in parts A and C normalized to the interelectrode distance B (Fig. 4, *c*). We found that the speed of eSPW propagation in a septal-temporal direction (215 ± 100 mm/s) does not significantly differ from the speed of eSPW propagation in the temporal-septal direction (259 ± 104 mm/s; $p > 0.05$). These values were slightly lower than the speed of SPW propagation in adult animals (~ 350 mm/s, [Patel et al., 2013]), but much higher than the speed of GDP propagation in the intact hippocampus in vitro (~ 7 – 10 mm/s, [Leinekugel et al., 1998]).

We also asked whether eSPW amplitude changes during their propagation along the hippocampus. To this aim, we compared the relative amplitudes of eSPWs generated in parts A and C at the proximal and distant recording sites. In both cases, propagating eSPWs showed a tendency to fade at the more distant site attaining $86 \pm 19\%$ of the amplitude at the proximal site in cases of septal-temporal propagation from part A, and $82 \pm 20\%$ in cases of temporal-septal propagation from part C but this difference was not significant ($p = 0.68$). These results indicate that eSPWs fade little during longitudinal propagation in both directions, at least within the distances explored here.

We performed analysis of MUA associated with eSPWs at the septal and intermediate segments of the hippocampus (Fig. 5). Normalized MUA peri-event time histograms (PETHs) triggered by septal eSPW onsets attained maximal values of $6.6 \pm 3.3\%$ spikes per ms (6.6 ± 1.3 -fold increase above baseline) and $4.7 \pm 1.5\%$ spikes per ms

(6.7 ± 3.0 -fold increase above baseline) with time lags of 72 ± 29 ms and 52 ± 13 ms ($p > 0.05$) in the septal and intermediate segments, respectively. The cross-correlation of MUA between the two recording sites within ± 1 s time window from the eSPW onset revealed no significant longitudinal time lag (-4.0 ± 7.1 ms), while the peak of the cross-correlation attained $2.1 \pm 0.8\%$ spikes per ms ($n = 4$ rats; Fig. 5, *b*). Thereby, eSPWs supported a high level of longitudinal synchronization of multiple unit activity. Separate MUA analysis during eSPWs originating in portions A and C failed to reveal a significant time difference of MUA at either of the electrodes, however (not shown), this could be due to a long-lasting increase in MUA through the time course of eSPW relative to the short time lags expected for the rapidly propagating eSPWs.

Discussion. Our main finding is that eSPWs are highly synchronized and support correlated neuronal activity along the septo-temporal hippocampal axis in rat pups in vivo. We found that nearly all eSPWs co-occur in the septal and intermediate hippocampal segments. Spatial-temporal analysis of eSPWs suggested that eSPWs are more often initiated in the septal regions of hippocampus than in the temporal regions, which is in keeping with the septal-temporal gradient in the neonatal rat hippocampus previously described in the intact hippocampus in vitro [Leinekugel et al., 1998]. This septal-temporal gradient was not observed in adult animals, where the probability of SPW-ripple occurrence is similar along the entire extent of the septo-temporal axis, indicating that each segment of the hippocampus can equally support both SPWs and ripples [Patel et al., 2013] suggesting that the septal-temporal gradient in eSPW initiation is a developmental phenomenon which is lost during maturation. The slightly lower velocity of the longitudinal eSPW propaga-

tion observed in the present study (~250 mm/s) compared to adult SPWs (~350 mm/s) is probably due to a slower axonal conduction velocity in the immature neurons and less developed CA3 recurrent network [Gomez-Di Cesare et al., 1998]. It is conceivable that longitudinal eSPW synchronization in CA1 hippocampus involves the longitudinal recurrent CA3 network which is the origin of adult SPWs [Buzsaki, 2015; Csicsvari et al., 2000; Ylinen et al., 1995], and which is also involved in generation of eSPWs in neonates in both septal and intermediate segments as manifested by a current sink of eSPWs in CA1 sr (Fig. 1), where CA3–CA1 synapses are located. In addition, longitudinal eSPWs synchronization may also involve synchronous inputs from the entorhinal cortex, which is evidenced by synchronous eSPW current sinks in the septal and intermediate segments in the CA1 sl-m, where synapses from the entorhinal cortex are located (Fig. 1, see also [Valeeva et al., 2019a]).

While the septal-temporal gradient in eSPW initiation is also characteristic of GDPs in the isolated hippocampus in vitro, the speed of GDP propagation is much slower (~7–10 mm/s) [Leinekugel et al., 1998] than that of eSPWs in vivo (~250 mm/s). The low speed of GDP propagation has been previously attributed to long and variable delays of spikes evoked by depolarizing GABA, which is importantly involved in generation of GDPs, and to the shunting effects of depolarizing GABA [Valeeva et al., 2010; Khalilov et al., 2015]. In keeping with this, blockade of GABAergic transmission transforms slowly propagating GDPs to fast propagating hypersynchronous, glutamate-driven epileptiform events [Khalilov et al., 1997; Lamsa et al., 2000; Valeeva et al., 2010], which are also evoked by GABA(A) receptor blockade in the neonatal hippocampus in vivo [Baram, Snead, 1990]. While the excitatory actions of GABA in the neonatal cortex in vivo are debated [Valeeva et al., 2016; Kirmse et al., 2015; Kirmse et al., 2018], these findings suggest that independently of whether GABA exerts depolarizing or hyperpolarizing actions, the roles of GABA at the network level remain mainly inhibitory in vivo and fast rate of eSPW propagation along the hippocampus mainly involves glutamatergic mechanisms including the CA3 recurrent circuit and synchronous entorhinal input as discussed above.

Conclusion. In conclusion, we have shown that longitudinal synchronization of activity in the hippocampal system emerges early during postnatal development (it is already present in the electrical activity of several days old rat pups) and that early longitudinal synchronization is supported by highly correlated eSPWs. Longitudinal synchronization of eSPWs likely contributes to the development of intrahippocampal synaptic connections by means of synchronization of neuronal activity and activity-dependent plasticity. Our results also provide further evidence that eSPWs are a developmental prototype of adult SPWs, which also display a high level of longitudinal synchrony [Patel et al., 2013; Buzsaki, 2015].

This work was supported by the subsidy No. 6.2313.2017/4.6 allocated to Kazan Federal University for the state assignment in the sphere of scientific activities, RFBR grant No. 17-04-02083 and was performed within the framework of the program of competitive growth of Kazan Federal University and collaborative agreement between the Institut National de la Santé et de la Recherche Médicale and Kazan Federal University (LIA to RK).

REFERENCES

- Akhmetshina, D., Nasretdinov, A., Zakharov, A., et al., "The nature of the sensory input to the neonatal rat barrel cortex," *J. Neurosci.*, **36**, 9922–9932 (2016).
- Baram, T. Z. and Snead, O. C., "Bicuculline induced seizures in infant rats: ontogeny of behavioral and electrocortical phenomena," *Dev. Brain Res.*, **57**, 291–295 (1990).
- Buhl, D. L. and Buzsaki, G., "Developmental emergence of hippocampal fast-field "ripple" oscillations in the behaving rat pups," *Neuroscience*, **134**, 1423–1430 (2005).
- Buzsaki, G., "Two-stage model of memory trace formation: a role for "noisy" brain states," *Neuroscience*, **31**, 551–570 (1989).
- Buzsaki, G., "Hippocampal sharp wave-ripple: A cognitive biomarker for episodic memory and planning," *Hippocampus*, **25**, 1073–1188 (2015).
- Chrobak, J. J. and Buzsaki, G., "Selective activation of deep layer (V–VI) retrohippocampal cortical neurons during hippocampal sharp waves in the behaving rat," *J. Neurosci.*, **14**, 6160–6170 (1994).
- Csicsvari, J., Hirase, H., Mamiya, A., and Buzsaki, G., "Ensemble patterns of hippocampal CA3–CA1 neurons during sharp wave-associated population events," *Neuron*, **28**, 585–594 (2000).
- Gomez-Di Cesare, C. M., Smith, K. L., Rice, F. L., and Swann, J. W., "Anatomical properties of fast spiking cells that initiate synchronized population discharges in immature hippocampus," *Neuroscience*, **75**, 83–97 (1996).
- Karlsson, K. A., Mohs, E. J., di Prisco, G. V., and Blumberg, M. S., "On the co-occurrence of startles and hippocampal sharp waves in newborn rats," *Hippocampus*, **16**, 959–965 (2006).
- Khalilov, I., Khazipov, R., Esclapez, M., and Ben-Ari, Y., "Bicuculline induces ictal seizures in the intact hippocampus recorded in vitro," *Eur. J. Pharmacol.*, **319**, R5–R6 (1997).
- Khalilov, I., Minlebaev, M., Mukhtarov, M., and Khazipov, R., "Dynamic changes from depolarizing to hyperpolarizing GABAergic actions during giant depolarizing potentials in the neonatal rat hippocampus," *J. Neurosci.*, **35**, 12635–12642 (2015).
- Khazipov, R., Zaynutdinova, D., Ogievetsky, E., et al., "Atlas of the postnatal rat brain in stereotaxic coordinates," *Front. Neuroanat.*, **9**, 161 (2015), doi: 10.3389/fnana.2015.00161.
- Kirmse, K., Hubner, C. A., Isbrandt, D., et al., "GABAergic transmission during brain development: Multiple effects at multiple stages," *Neuroscientist*, **24**, 36–53 (2018).
- Kirmse, K., Kummer, M., Kovalchuk, Y., et al., "GABA depolarizes immature neurons and inhibits network activity in the neonatal neocortex in vivo," *Nat. Commun.*, **6**, 7750 (2015).
- Lamsa, K., Palva, J. M., Ruusuvuori, E., et al., "Synaptic GABA(A) activation inhibits AMPA-kainate receptor-mediated bursting in the newborn (P0–P2) rat hippocampus," *J. Neurophysiol.*, **83**, 359–366 (2000).
- Leinekugel, X., Khalilov, I., Ben-Ari, Y., and Khazipov, R., "Giant depolarizing potentials: the septal pole of the hippocampus paces the activity of the developing intact septohippocampal complex in vitro," *J. Neurosci.*, **18**, 6349–6357 (1998).
- Leinekugel, X., Khazipov, R., Cannon, R., et al., "Correlated bursts of activity in the neonatal hippocampus in vivo," *Science*, **296**, 2049–2052 (2002).

- Marguet, S. L., Le-Schulte, V. T., Merseburg, A., et al., "Treatment during a vulnerable developmental period rescues a genetic epilepsy," *Nat. Med.*, **21**, 1436–1444 (2015).
- Mohs, E. J. and Blumberg, M. S., "Synchronous bursts of neuronal activity in the developing hippocampus: modulation by active sleep and association with emerging gamma and theta rhythms," *J. Neurosci.*, **28**, 10134–10144 (2008).
- Mohs, E. J., Karlsson, K. A., and Blumberg, M. S., "Developmental emergence of transient and persistent hippocampal events and oscillations and their association with infant seizure susceptibility," *Eur. J. Neurosci.*, **26**, 2719–2730 (2007).
- Patel, J., Schomburg, E. W., Berenyi, A., et al., "Local generation and propagation of ripples along the septotemporal axis of the hippocampus," *J. Neurosci.*, **33**, 17029–17041 (2013).
- Suzuki, S. S. and Smith, G. K., "Spontaneous EEG spikes in the normal hippocampus. I. Behavioral correlates, laminar profiles and bilateral synchrony," *Electroencephalogr. Clin. Neurophysiol.*, **67**, 348–359 (1987).
- Valeeva, G., Abdullin, A., Tyzio, R., et al., "Temporal coding at the immature depolarizing GABAergic synapse," *Front. Cell. Neurosci.*, **4** (2010).
- Valeeva, G., Janackova, S., Nasretdinov, A., et al., "Emergence of coordinated activity in the developing entorhinal-hippocampal network," *Cereb. Cortex*, **29**, 906–920 (2019a).
- Valeeva, G., Nasretdinov, A., Rychkova, V., and Khazipov, R., "Bilateral synchronization of hippocampal early sharp waves in neonatal rats," *Front. Cell. Neurosci.*, **13**, 29 (2019b).
- Valeeva, G., Tressard, T., Mukhtarov, M., et al., "An optogenetic approach for investigation of excitatory and inhibitory network GABA actions in mice expressing channelrhodopsin-2 in GABAergic neurons," *J. Neurosci.*, **36**, 5961–5973 (2016).
- Ylinen, A., Bragin, A., Nadasdy, Z., et al., "Sharp wave associated high-frequency oscillation (200Hz) in the intact hippocampus: network and intracellular mechanisms," *J. Neurosci.*, **15**, 30–46 (1995).